UNCERTAINTY EVALUATION THROUGH SIMULATIONS OF VIRTUAL ACQUISITIONS MODIFIED WITH MECHANICAL AND ELECTRICAL ERRORS IN A CYLINDRICAL NEAR-FIELD ANTENNA MEASUREMENT SYSTEM

S. Burgos, M. Sierra-Castañer, F. Martín, J.L. Besada
Universidad Politécnica de Madrid. E.T.S.I. de Telecomunicación
Ciudad Universitaria, 28040 Madrid, Spain
E-mail: sarab@gr.ssr.upm.es, m.sierra.castaner@gr.ssr.upm.es, fmartin@gr.ssr.upm.es, besada@gr.ssr.upm.es

ABSTRACT

An error simulator based on virtual cylindrical near-field acquisitions has been implemented in order to evaluate how mechanical or electrical inaccuracies may affect the antenna parameters. In outdoor ranges, where the uncertainty could be rather important due to the weather conditions, an uncertainty analysis a priori based on simulations is an effective way to characterize measurement accuracy. The tool implemented includes the modelling of the Antenna Under Test (AUT) and the probe and the cylindrical near-to-far-field transformation. Thus, by comparing the results achieved considering an infinite far-field and the ones obtained while adding mechanical and electrical errors, the deviations produced can be estimated. As a result, through virtual simulations, it is possible to determine if the measurement accuracy requirements can be satisfied or not and the effect of the errors on the measurement outcomes can be checked. Several types of results were evaluated for different antenna sizes, which allowed determining the effect of the errors and uncertainties in the measurement for the antennas under study.

Keywords: cylindrical near-field acquisition, mechanical and electrical errors, uncertainty, directivity.

1. Introduction

In order to evaluate how mechanical or electrical errors may affect in the main antenna parameters − i.e. radiation patterns, directivity, Side Lobe Levels (SLL), beam width, maximum and null position −, an error simulator based on virtual acquisitions of the measurement of the radiation characteristics in a cylindrical near-field facility has been implemented [1], [2]. In this case, the AUT is modelled as an array of vertical dipoles and the probe is assumed to be a corrugated horn antenna. This tool allows simulating an acquisition containing mechanical errors – deterministic and random errors in the *x*-, *y*- and *z*-position – and also electrical inaccuracies – such as phase errors or White Gaussian Noise –. Then, after a near-to-far-field transformation [3], by comparing the results obtained in the ideal case and when including errors, the deviation produced can be estimated. As a result, through virtual simulations, it is possible to determine if the measurement accuracy requirements can be satisfied or not and the effect of the errors on the measurement results can be checked. This paper describes the error simulator implemented and the results achieved for some of the error sources considered for L-band RADAR antennas in a 15meters cylindrical near field system.

2. Description of the error simulator for the inaccuracies evaluation

Since the system analyzed is an outdoor system, there are some error sources more relevant than others. Actually, the effects of the wind for the probe positioning and the temperature changes affecting the phase response of the cables can be significant and thus have to be analyzed. With this scenario, an uncertainty analysis a priori based on simulations was chosen. As a result, the strategy adopted to evaluate the sources of error is to simulate these deviations and to examine the influence that they have in the final results. The first step to evaluate how errors could affect the final results is to model the transmitting and the receiving antennas and to simulate the acquisition process including errors. Then, the far-field radiation pattern is obtained by applying a near-to-far-field transformation. Finally, the simulator compares the outcomes achieved from the reference data (i.e. an infinite far-field) with the ones including deviations.

A probe correction was applied to achieve the far-field and therefore the received field was calculated taking into account the field radiated by all the dipoles modified by the probe pattern. The field from a dipole in each point of the grid is given by the sum of three spherical waves [4]. The probe is an ideal conical corrugated horn (keeping $\mu=\pm1$) characterized by the calculated radiation pattern of the main planes. For this investigation, two AUT were evaluated: the first is 5.3meters long and 2.1meters high and the second is 2.7meters long and 1meter high. Besides, the AUT radiating elements are $\lambda/2$ dipoles vertically displaced over a ground plane at a distance

equal to λ/4, and assumed to be infinite, so "Image Theory" can be applied.

In addition, a uniform column and row excitation in amplitude and phase is considered, the distance from AUT to probe is 5meters, the vertical path of the probe is 15meters and the frequency selected is 1215MHz.

3. Error simulator for computational, mechanical and electrical errors

Simulator validation

To validate the algorithm, the array infinite far-field of the antenna (product of array factor by the radiation element pattern) is compared with the far-field calculated through the cylindrical near-field acquisition. This comparison is also useful to confirm that the elevation range is valid. **Figure 1** and **Figure 2** show the results achieved.

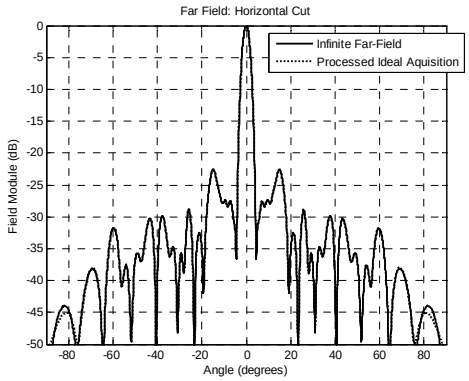

Figure 1: Horizontal cut: infinite far-field versus ideal acquisition

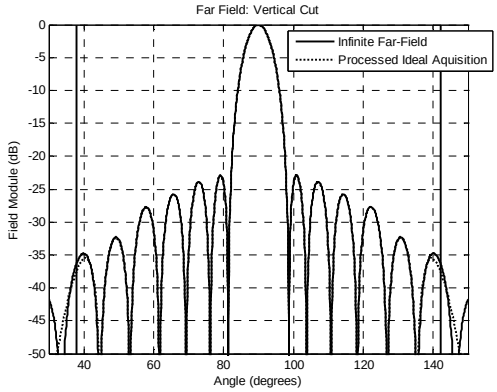

Figure 2: Vertical cut: infinite far-field versus ideal acquisition

The diagrams obtained showed a very good agreement between both radiation patterns and the validity of the angular margin of the measurement was confirmed. It should be noted that the small discrepancies in the extremes of the horizontal angular range are due to the approximation of the acquisition model.

Truncation errors

To estimate the truncation error, the angular range indicated in [5] and [6] is compared with the angular range obtained to have an error (difference between the infinite far-field and the processed acquisition) lower than 0.5dB. This evaluation was performed with the two antennas varying the probe tower height, as shown in **Table 1** and **Table 2**.

Antenna1: 5.3meters x 2.1meters		
	$\theta_0 = \tan^{-1}\frac{\mathbf{L_z - D}}{2\mathbf{x_0}}$,[5,6]	**Difference between radiation patterns < 0.5 dB**
Lz (meters)	**$\pm\theta_0$ (degrees)**	**θ_1 (degrees)**
15	± 52.2	± 49.2
12	± 44.7	± 40.6
9	± 34.6	± 31.6
6	± 21.3	± 16.7

Table 1. Truncation error evaluation with Antenna 1 (Larger antenna)

Antenna2: 2.7meters x 1meter		
	$\theta_0 = \tan^{-1}\frac{\mathbf{L_z - D}}{2\mathbf{x_0}}$,[5,6]	**Difference between radiation patterns < 0.5 dB**
Lz (meters)	**$\pm\theta_0$ (degrees)**	**θ_1 (degrees)**
15	± 54.4	± 51.7
12	± 47.6	± 44.6
9	± 38.5	± 35.4
6	± 26.4	± 20.5

Table 2. Truncation error evaluation with Antenna 2 (Smaller antenna)

From these results it is clear that the formula of the first column slightly overestimates the valid angular range.

Pointing errors

There are two different sources of deterministic errors that affect the AUT pointing: the axis non parallelism and the determination of the zero position of the azimuthal direction (in this case, the random errors caused by the wind effect are not considered). Both inaccuracies are directly translated to the error pointing, and they could be evaluated and corrected to minimize them. While the axis non parallelism can be measured with an optical procedure (i.e. laser tracker), the zero position of the azimuthal direction depends on the RADAR positioner encoder and the triggering of the vector network analyzer that can be either calculated or measured. Therefore, both errors can be compensated with a rotation of the electric field [7], and as a result they are omitted for this study.

Mechanical errors in positioning system

To evaluate the effects of the mechanical errors on the outcomes, mainly due to the windy outdoor conditions, some simulations were performed including systematic and random errors in each sample in *x*, *y* and *z* directions.

The simulations were carried out for different peak to peak error amplitudes (from ±0.05λ to ± 0.2 λ).

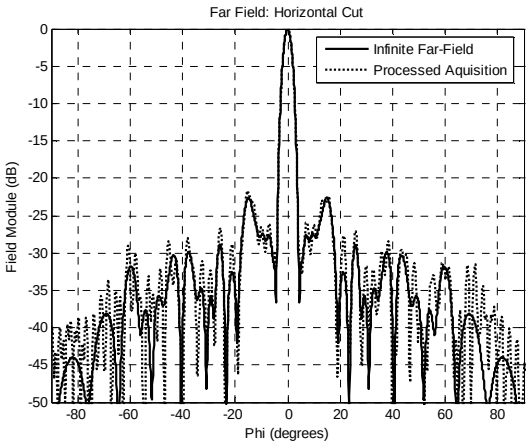

Figure 3: Horizontal cut including a random error in *x*-position of the probe axis (± 0.05λ mm)

It was clearly seen the noticeable influence of the errors on the main planes of the far-field radiation pattern, as **Figure 3** shows. In addition, since the directivity is one of the most characteristic figures-of-merit that can describe the behaviour of an antenna, a detailed investigation has been carried out to evaluate how the mechanical errors may influence the directivity. In the simulations performed, the directivity was calculated when including a systematic error with the shape of a slope in the *x*-position of the probe, a sinusoidal systematic error in the *x*-position of the probe, a uniform random error in the *x*-, *y*- and *z*-position of the probe. In this case, 10 iterations were carried out for each of the peak to peak error amplitude.

For the random error in *x*-, *y*- and *z*-probe the mean and standard deviation of the error introduced in the directivity were achievable. From the results achieved, it was noticed that as expected the magnitude of the error in the directivity increase while augmenting the error introduced in the acquisition process, as **Figure 4** and **Figure 5** illustrates.

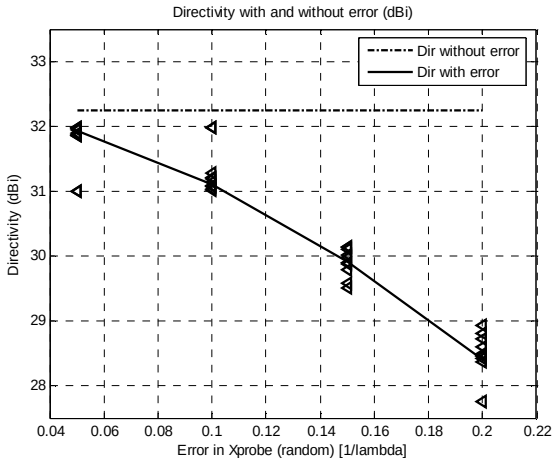

Figure 4: Effect of a random error in the *x*-position of the probe on the directivity

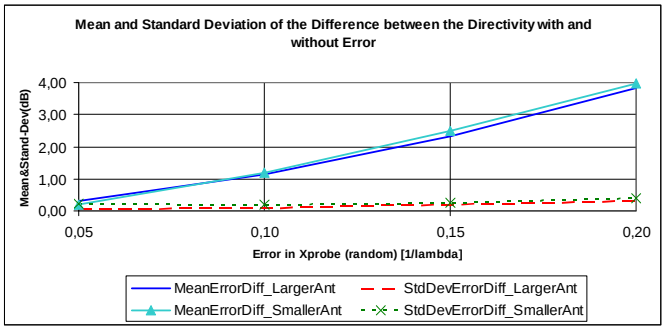

Figure 5: Mean and σ of the difference between the directivity with and without random error in the *x*-position of the probe for the two antennas

It should be noted that the increase in the mean and in the standard deviation is almost the same for the two antenna sizes.

Phase errors

The temperature variations during the acquisition process may cause phase errors in the near-field acquired. The study carried out establishes the influence that this inaccuracy may induce on the radiation pattern and directivity. As a representative example of the results achieved, **Figure 6** illustrates the effect of the random phase error in the directivity when increasing the error magnitude. In the figure, the broken line indicates the directivity without error, the triangles represent the directivity with error for each individual simulation and the line shows the average value of the directivity with error. Since several simulations were performed for each phase error, the mean and the standard deviations (σ) of the error in the directivity were calculated, as **Figure 7** shows.

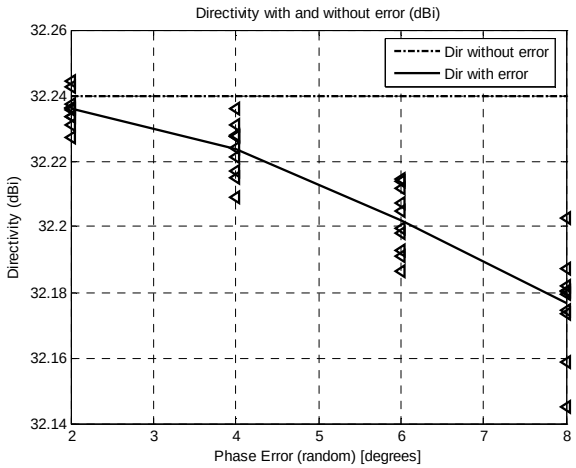

Figure 6: Effect of a random error in phase on the directivity

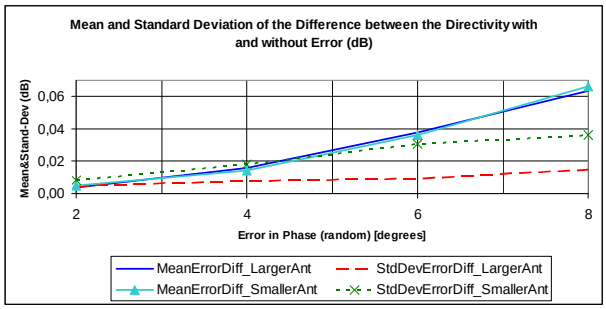

Figure 7: Mean and σ of the difference between the directivity with and without random phase error for the two antenna

Once more, it could be observed, that the mean and the standard deviation of the error increase while the phase error introduced in the acquired field becomes larger. In addition, it should be noted that in this case the uncertainty introduced by the phase error is larger when the antenna is smaller.

Errors due to a White Gaussian Noise

In order to evaluate the effect of the noise in the antenna parameter, a White Gaussian Noise has been added to each value of the acquired field with respect to the maximum. Then, the same procedure as for the previous error sources has been applied. **Figure 8** and **Figure 9** represent the results achieved:

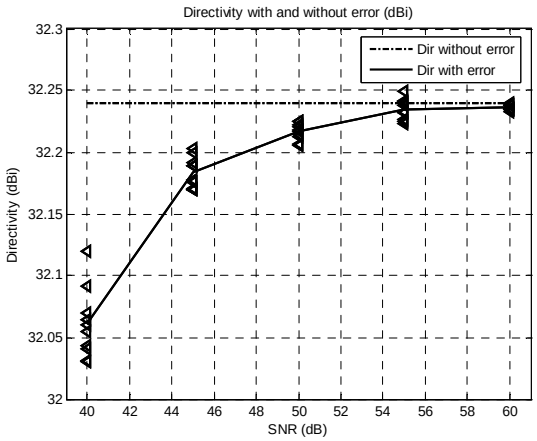

Figure 8: Effect of the noise on the directivity

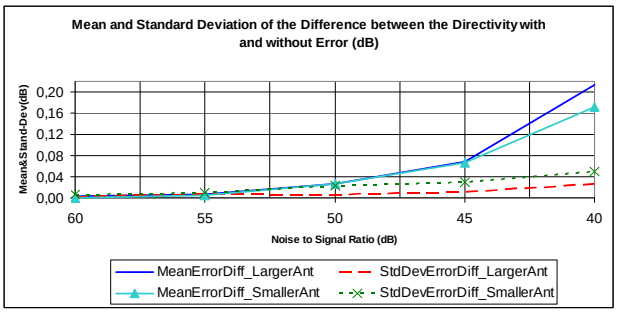

Figure 9: Mean and σ of the difference between the directivity with and without random error due to a White Gaussian Noise for the two antennas

From these outcomes, it is noteworthy that the mean and the standard deviation of the error in the directivity exponentially increase while augmenting the noise. Furthermore, the uncertainty introduced by the noise is slightly larger when the antenna is smaller.

4. Error analysis based on Montecarlo simulations

Typical calculation of errors in antenna measurements is based on the calculation or estimation of the standard deviation of each error term and the application of the central limit theorem for the combined uncertainty. In this particular case, a Montecarlo study with one hundred iterations per antenna excitation was implemented. The Montecarlo simulations were carried out in order to establish how the residual errors due to inaccuracies could affect the final outcomes.

The antenna simulated was 5.3metres long and 2.1meters high, the antenna and the probe were separated a distance equal to 5metres, the probe tower was 15.5metres high and the valid angular range of the measurement results was from -20.9degrees to 123.2degrees. In addition, the next deviations were added in the near-field acquisition: a random error of ±1millimetre in the *x*- and *y*-position of the probe, a random error of ±0.5millimetre in the *z*-position of the probe, a phase error of ±1degree and a noise considering a signal to noise of 75dB with respect to the maximum. In this study the inaccuracies in the main parameters of the antenna −directivity, pointing directions, SLL and beamwidth − were calculated.

Besides, it is worth noting that for this case, different amplitude distribution – sum and difference diagrams, electric tilt… – were examined:

- Sum amplitude distribution in the horizontal and in the vertical planes,
- Sum amplitude distribution in the horizontal plane and difference amplitude distribution in the vertical plane,
- Difference amplitude distribution in the horizontal plane and sum amplitude distribution in the vertical plane.

These cases were studied with the antenna mechanically tilted 16.08 degrees from the vertical axis and with electrical tilt of 0degrees or 40degrees in the vertical plane. As said before, the results obtained with the simulator show the comparison between the ideal far-field radiation pattern with the far-field radiation pattern including errors. In the representation of the results 100 lines, one for each simulated measurement. In this analysis, the probe correction was not included to reduce the computational time of the simulations. In **Figure 10**, **Figure 11** and **Figure 12** the following figures, some

diagrams of the far-field achieved with the antenna in these scenarios.

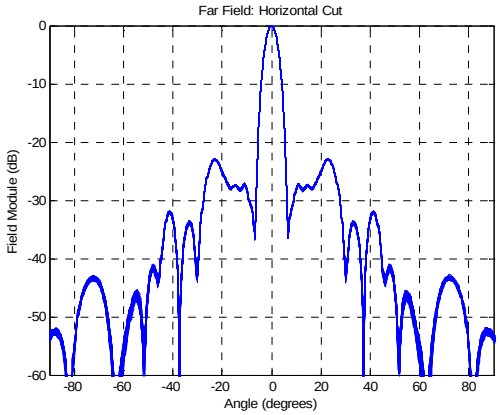

Figure 10: Comparison simulations with and without errors: Horizontal Cut, Sum amplitude distribution, 100 iterations

From the graphs, it could be noticed that the outcomes are valid over the angular range expected. Furthermore it is remarkable that the errors are particularly significant at the noise level (75 dB of S/N), as it was expected.

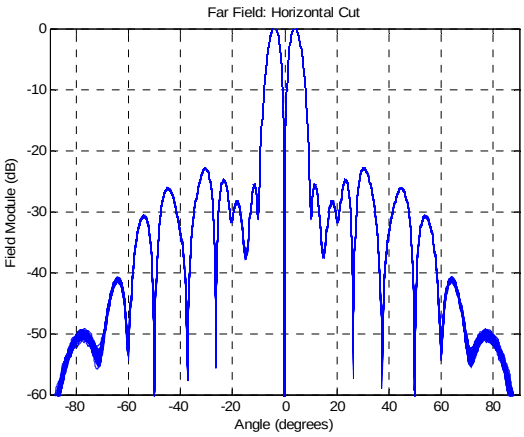

Figure 11: Comparison simulations with and without errors: Horizontal cut, Difference amplitude distribution, 100 iterations

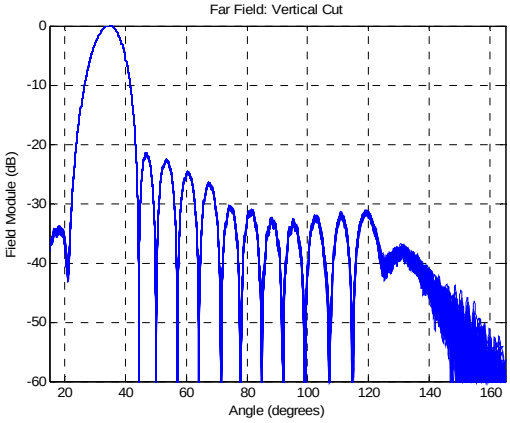

Figure 12: Comparison simulations with and without errors: Vertical cut, Sum amplitude distribution, 100 iterations

The simulator also represents the histograms of the error in the different antenna parameters. For instance, **Figure 13**, **Figure 14** and **Figure 15** show the histograms of the sum diagram distribution, which allows determining the probability distribution of the errors.

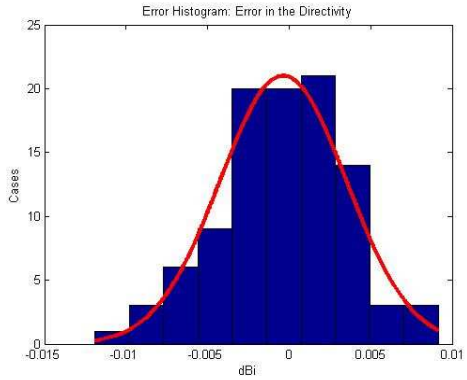

Figure 13: Histogram of the error in the directivity

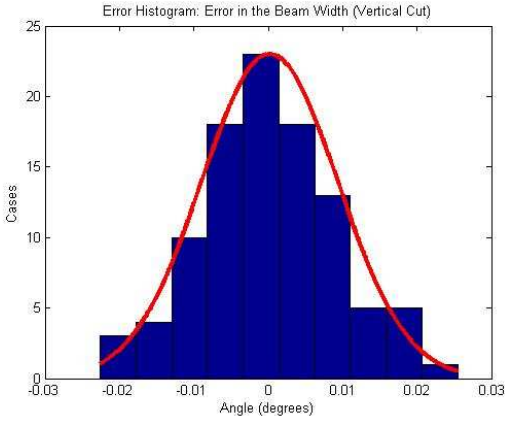

Figure 14: Histogram of the error in the beam width in the vertical cut

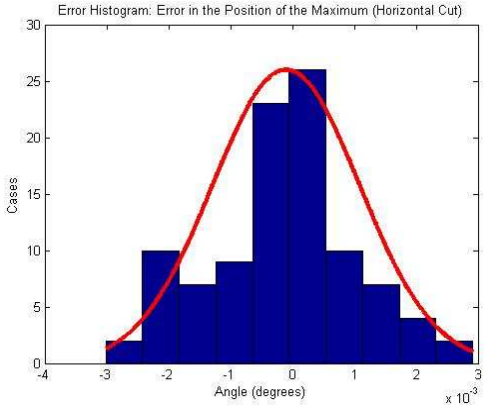

Figure 15: Histogram of the error in the position of the maximum in the horizontal cut

In addition, the Montecarlo study was completed with the statistical analysis achieved from the 100 iterations. **Table 3** summarizes the results obtained when no electrical tilt is considered.

PARAMETER	QUANTITY	RMS ERROR	MAXIMUM ERROR
Directivity (dBi)	32.24	$1.86\ 10^{-4}$	0.0044
Beam Width in the Horizontal Cut (degrees)	3.28	$3.91\ 10^{-4}$	$9.5\ 10^{-4}$
Beam Width in the Vertical Cut (degrees)	6.93	$2.48\ 10^{-4}$	0.0065
SLL (-20 dB to -30 dB)	–	–	0.5 dB
SLL (-30 dB to -40 dB)	–	–	1.5 dB
Position of the maximum in the Horizontal Cut (degrees)	0	$1.07\ 10^{-4}$	0.0030
Position of the maximum in the Vertical Cut (degrees) for the sum pattern	73.92	$2.94\ 10^{-4}$	0.0084
Position of the null in the Vertical Cut (degrees) for the difference pattern	73.92	$2.74\ 10^{-4}$	0.0062

Table 3: Statistical results of the Montecarlo study

5. Conclusion

A simulator has been implemented for evaluating the influence of mechanical and electrical errors in the measurement antenna parameters of the AUT in a cylindrical near field antenna measurement system. The simulator allows introducing deterministic and random errors and after a near-to-far-field transformation the different radiation parameters − radiation patterns, directivity, beam width, position of the maximum − can be calculated. Therefore, this tool allows not only to quantify a priori the value of the systematic error and the uncertainty introduced in the measurement system but also to evaluate the limits of the accuracy in the antenna measurements according to the kind of antenna and the mechanical and electrical performances of the systems. In addition, through Montecarlo simulations, it is possible to establish the probability distribution of the errors.

6. References

[1] F. Martín Jiménez, S. Burgos Martínez, M. Sierra Castañer, J.L. Besada, "*Design of a Cylindrical Near Field System for RADAR antennas*", Proceedings of the 1st EuCap Conference, Nize, November 2006.

[2] S. Burgos Martínez, F. Martín Jiménez, M. Sierra Castañer, J.L. Besada, "*Error Estimator in Cylindrical Near Field System for large RADAR antennas*", Proceedings of the 1st EuCap Conference, Nize, November 2006.

[3] W. M. Leach, Jr., D. T. Paris, "*Probe Compensated Near-Field Measurements on a Cylinder*", IEEE Transactions on Antennas and Propagation, Vol. AP-21, No.4, pp. 435-445, July 1973.

[4] Robert S. Elliot, "*Antenna Theory and Design*", Ed. Prentice-Hall, Inc., Englewood Cliffs, New Jersey.

[5] A. D. Yaghjian, "*Upper-bound errors in far-field antenna parameters determined from planar near-field measurements, Part 1: Analysis*", Nat. Bur. Stand., and Tech. Note 667, 1975.

[6] A. C. Newell and M. L. Crawford, "*Planar near-field measurements on high performance array antennas*", Nat. Bur. Stand., NBSIR 74-380, July 1974.

[7] Y. Rahmat-Samii, "*Useful Coordinate Transformations for Antenna Applications*", IEEE Transactions on Antennas and Propagation, Vol. AP-27, No. 4, pp. 571-574, July 1979.